Available online at www.sciencedirect.com
ScienceDirect
Journal of Power Sources 175 (2008) 288–295
JOURNAL OF POWER SOURCES
www.elsevier.com/locate/jpowsour

A study of process parameters of LSM and LSM–YSZ composite cathode films prepared by screen-printing

Jinhua Piao [b], Kening Sun [a,b,*], Naiqing Zhang [b], Shen Xu [b]

[a] *Department of Materials Science and Engineering, Beijing Normal University, Beijing 100875, China*
[b] *Department of Applied Chemistry, Harbin Institute of Technology, Harbin 150001, China*

Received 29 July 2007; received in revised form 21 September 2007; accepted 21 September 2007
Available online 2 October 2007

Abstract

A screen-printing technique was developed to fabricate porous cathode film for solid oxide fuel cells. Several key process parameters such as the selection of binders, the mesh of screen, sintering temperature and sintering time were investigated and reported. SEM results showed that the selected process parameters exerted obvious influences on the structure of the screen-printed cathode film. Impedance spectra data were used to evaluate the performance of cathode films made by different process parameters. The optimized process parameters were as follows: ethyl cellulose used as a binder, 120 mesh screen-printing sintering at 1200 °C for 2 h. Based on the optimized parameters, the polarization resistance of pure LSM cathode was 0.396 Ω cm^2 at 800 °C; the LSM–YSZ composite cathode displayed R_p value of 0.2027 Ω cm^2 at 850 °C, 0.2463 Ω cm^2 at 800 °C and 0.5168 Ω cm^2 at 750 °C, respectively. The performance of the LSM–YSZ composite cathode improved significantly after being polarized at 300 mA cm^{-2} and 800 °C for 150 h. After 150 h, the over-potential of the composite cathode was stable.

Keywords: SOFC; Cathode; Process parameter; Screen-printing; Impedance spectra

1. Introduction

In recent years, there has been an intense focus to develop solid oxide fuel cells (SOFCs), which are capable of delivering high energy at reduced temperatures [1]. For intermediate temperature planar anode-supported cells, the resistance of electrolyte has been reduced to acceptable (or negligible) levels but the performance of the electrodes, especially at the cathode, becoming the limiting factor. Theoretical and experimental work has shown that the dominant loss was attributed to the cathode in the cell operating at the range of 600–850 °C [2–4]. There are two approaches to resolve this concern. One is to develop new cathode materials with higher performance than conventional strontium-doped lanthanum manganites ($La_{1-x}Sr_xMnO_3$, LSM) cathode materials, such as $La_xSr_{1-x}Fe_yCo_{1-y}O_3$ [5,6]. The other method is to optimize the microstructure of the LSM cathode [7,8]. Recently, there has been significant progress in the development of intermediate temperature anode-supported SOFCs with conventional LSM cathode. For example, de Souza et al. [9] reported that a thin-film SOFC with a yttria-stabilized zirconia (YSZ) electrolyte of ∼10 μm, a Ni/YSZ anode and a LSM-based cathode could achieve a high power density of ∼1.8 W cm^{-2} at 800 °C.

To improve the performance of the cathode, many groups have studied the relationship between the cathode microstructure and the electrochemical performance [10,11]. The electrode microstructure is controlled by several factors, such as the thickness of the cathode film, the particle size of electrode materials and the sintering conditions [7,12]. Choi et al. [7] reported that the LSM (mean diameter of 1.54 μm) showed a favorable activity in the initial stage, but this activity declined quickly. When the particle size was 11.31 μm, the LSM cathode possessed unsatisfactory initial activity, but this activity was quite stable due to a negligible change in the microstructure. A trade-off between the number of active sites and the particle growth rate was likely made at the intermediate size (about 5 μm) [7]. JØrgensen et al. [11] reported that the electrode microstructure was found to be less dense and contained smaller grains with the sintering temperature decreasing in the range from 1300 °C to 1150 °C. This resulted in a decrease in polarization resis-

* Corresponding author. Tel.: +86 451 86412153; fax: +86 451 86412153.
E-mail address: sunkn@hit.edu.cn (K. Sun).

0378-7753/$ – see front matter © 2007 Elsevier B.V. All rights reserved.
doi:10.1016/j.jpowsour.2007.09.078

tance with the corresponding sintering temperature decreasing. It has been generally accepted that the electrochemical performance of SOFC cathodes can be improved by mixing the cathode materials with electrolyte materials to increase the three-phase boundary (TPB) sites. Murray and Barnett [13] reported that the polarization resistance of LSM–YSZ50 composite cathode was 1.31 $\Omega\,cm^2$ at 750 °C under open circuit on YSZ electrolyte substrate. It was lower than the polarization resistance of pure LSM cathode (3.5 $\Omega\,cm^2$). This result showed that composite cathodes have better performance than pure cathodes since the TPB could be extended three-dimensionally into the composite cathode [10,13–16].

The screen-printing technique is one of the most important methods to fabricate cathode film. Process parameters may affect the electrochemical active area, the electronic conductivity of the electrodes and the gas diffusion for the reactants. However, reports related to the influences of the process parameters on microstructure and performance of screen-printing LSM and LSM–YSZ composite cathode films were insufficient. In this work, the effects of several important process parameters comprising of the selection of binders, the mesh of screen, sintering temperature and sintering time were studied.

2. Experimental

The $La_{0.8}Sr_{0.2}MnO_3$ (LSM) powders were prepared as the cathode materials for SOFCs by the co-precipitation method. $Mn(NO_3)_2{\cdot}6H_2O$, $La(NO_3)_2{\cdot}6H_2O$ and $Sr(NO_3)_2$ (all with a purity level of >99.9%, Gansu rare earth) were dissolved with the stoichiometric composition into water and then titrated into $NH_4HCO_3/NH_3{\cdot}H_2O$ buffer solution which was stirred constantly. The co-precipitated products were washed by deionised water and dispersed in *n*-butanol, then azeotropic distilled to obtain the LSM precursors. The precursors were subsequently heated at 1000 °C for 2 h to obtain the LSM powders.

A YSZ (Tosoh, Japan) electrolyte pellet was prepared by being sintered at 1550 °C for 6 h with the size of 15 mm in diameter and 0.6 mm in thickness. Three-electrode setup was used to measure the electrochemical performance. The LSM powders were made into slurry by being mixed with 1 mass% binder (ethyl cellulose or polyvinyl-butyral) and organic solvent (terpineol). For the composite cathode, 80 wt% LSM and 20 wt% YSZ (30 wt% sintered at 700 °C for 2 h and 70 wt% un-sintered YSZ) powders were mixed homogeneous and made into slurry. The slurries were screen-printed (The mesh material was silk) onto one side of the electrolyte pellet before being sintered at different temperatures to prepare cathode (WE). The cathode area was 5 mm × 5 mm. A commercial Pt paste (PC-Pt-7840, sino-platinum metals) was painted on the cathode side as reference electrode (RE) and painted to the other side of the electrolyte pellet as the counter electrode (CE) (Fig. 1). The counter area was 7 mm × 7 mm. The Pt electrodes were fired at 850 °C for 30 min. The electrochemical performance of the cells was measured using a potentiostat/galvanostat (model PARSTAT® 2273, Princeton applied research). The impedance frequency range was 10 mHz to 10^5 Hz with a signal amplitude of 5 mV. The impedance fitting analysis was controlled with software (Zsimpwin). The microstructures of the surface and the interface between cathode and electrolyte were studied by scanning electron microscopy (SEM, HITACHI, S-4700).

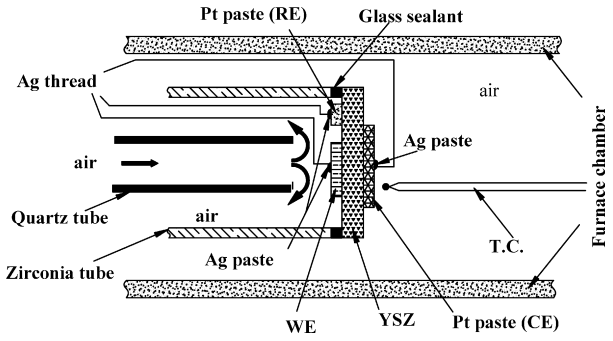

Fig. 1. Holder of three-electrode setup for high temperature electrochemistry measurement.

3. Results and discussions

3.1. Selection of binder for screen-printing slurry

The LSM cathode powders were made into slurry by being mixed with the binder and organic solvent before screen-printing. The selection of the binders would influence the microstructure of the cathode film. The binders for screen-printing cathode, ethyl cellulose and polyvinyl-butyral were evaluated. The fabricating process parameters were listed in Table 1 (sample A for ethyl cellulose as binder and sample B for polyvinyl-butyral as binder). The microstructures of the electrode films were measured by SEM (Fig. 2). It can be read-

Table 1
Process parameters for fabricating cathode films and impedance spectra data (measured at 800 °C)

Sample	Binder	Mesh screen	Sintering temperature (°C)	Sintering time (h)	Series resistance R_s ($\Omega\,cm^2$)	Polarization resistance R_p ($\Omega\,cm^2$)
A	Ethylcellulose	120	1200	2	0.8365	0.3961
B	Polyvinyl-butyral	120	1200	2	0.9567	0.7113
C	Ethylcellulose	100	1200	2	0.9577	0.8214
D	Ethylcellulose	140	1200	2	0.8576	0.909
E	Ethylcellulose	120	1150	2	1.11	0.95
F	Ethylcellulose	120	1250	2	1.261	0.851
G	Ethylcellulose	120	1300	2	1.237	1.205
H	Ethylcellulose	120	1200	1	0.899	1.0965
I	Ethylcellulose	120	1200	3	0.95	0.767

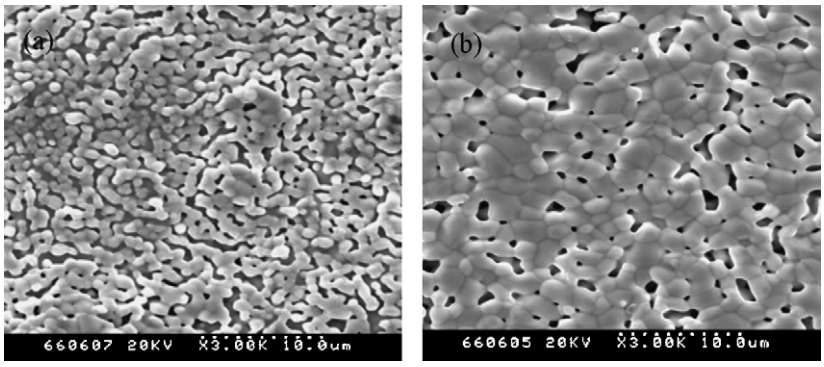

Fig. 2. SEM photos of LSM cathode films fabricated using different binders: (a) ethyl cellulose, (b) polyvinyl-butyral.

ily observed that the electrode film had a homogeneous pore size distribution when using the ethyl cellulose acted as the binder (Fig. 2(a)). The porosity was about 30–40% (estimated from SEM). The sample using polyvinyl-butyral as the binder showed that the film was dense and the porosity was only about 10% (Fig. 2(b)). The porosity would affect the performance of cathode significantly. This is because ethyl cellulose is a linear polymer, while polyvinyl-butyral has branches in its structure. Ethyl cellulose was considered to be the preferable binder to obtain fine and uniform microstructures because of its linear structure. From the polarization resistance (R_p) of samples A and B in Table 1 (resistance data obtained by impedance analysis at 800 °C), the same results were found. The sample of cathode film made by ethyl cellulose possessed lower R_p than the sample made by polyvinyl-butyral. The ohmic resistance (R_s) of sample A was also lower than in sample B. Because of the electrolyte, the counter electrode and reference electrode were identical; it can be considered that the increase of R_s resulted from the increase of interfacial resistance between the cathode and electrolyte. Polarization resistance R_p consists of the charge-transfer resistance R_{ct} and diffusion resistance R_d [17,18]. The R_{ct} of sample B (0.4949 Ω cm^2) was also higher than sample A (0.3111 Ω cm^2). The R_d of sample B was 0.2164 Ω cm^2, while the R_d of sample A was 0.085 Ω cm^2 (data from impedance fitting analysis). The decrease of R_{ct} and R_d in sample A was due to the increase of TPB sites and the higher porosity, respectively. The increase of R_s and R_p could have resulted from the effect of binder because all other conditions were same.

3.2. The effect of mesh screen amount

The mesh screen amount is critical for preparing porous cathode using the screen-printing technique. The mesh screen amount can significantly influence the microstructure of the film. In this section, we investigated the effect of mesh screen amount on the LSM cathode electrochemical performance. The Fig. 3 showed the SEM photos of cathode surfaces fabricated by different mesh screens. It can be found that films made by 100 mesh screen and 140 mesh screen both possessed more inhomogeneous pores than film made by 120 mesh screen (Fig. 2(a)). All the porosity was lower than 10%. From Table 1, it is clear that the R_p of the sample made by 120 mesh screen was the lowest (0.396 Ω cm^2). The R_{ct} of the sample C (0.64 Ω cm^2) and sample D (0.679 Ω cm^2) were both higher than that of sample A (0.3111 Ω cm^2). The R_d possessed same trend as R_{ct}. The R_d of sample C and sample D was 0.1814 Ω cm^2 and 0.2297 Ω cm^2, respectively. Both of them were higher than that of sample A (0.085 Ω cm^2). This attributed to the decrease of TPB sites because of inhomogeneous pores distribution and lower porosity.

3.3. The effect of sintering temperature and sintering time

The sintering temperature dramatically affects the microstructure of the electrodes. Fine porosity and fine-grained microstructure are desirable for the interface between the electrolyte and cathode to provide sufficient triple phase

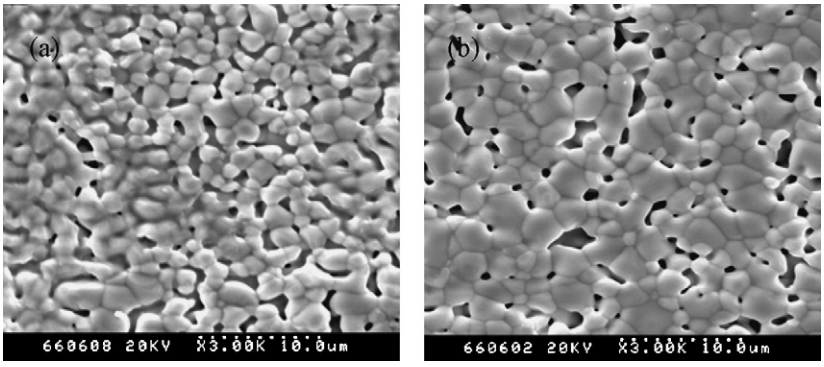

Fig. 3. SEM photos of LSM cathode films fabricated using different mesh screens: (a) 100 mesh, (b) 140 mesh.

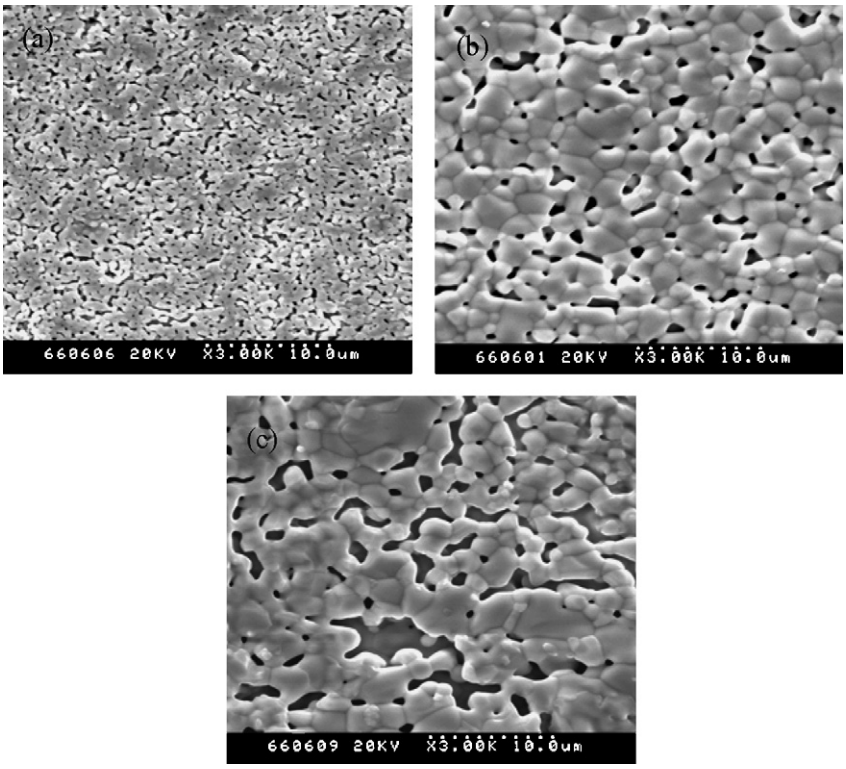

Fig. 4. SEM photos of LSM cathode films sintered at different temperatures: (a) 1150 °C, (b) 1250 °C, (c) 1300 °C.

boundaries for the oxidant electrochemical reduction [19,20]. Fig. 4 showed the photos for cathode films sintered at temperature between 1150 °C and 1300 °C (sample A (photo in Fig. 2(a)), E–G, Table 1). It can be noted that finer pores and smaller particles can be obtained in cathode film when the sintered temperature decreased. This trend was consistent with the report of JØrgensen et al. [11]. Larger particle size would reduce the TPB sites and influence performance. The surface of sample F (sintered at 1250 °C, Fig. 4(b)) possessed low porosity (lower than 10%). The dense cathode film can decrease the TPB sites and limit gas access to the TPB sites, leading to R_p increase. The surface of the sample G (sintered at 1300 °C, Fig. 4(c)) displayed inhomogeneous pore size distribution. LSM particles were partial aggregation and partial detachment, which not only decreased the porosity but also reduced the TPB length, which then limited the gas transport to TPB sites. This restrained the oxygen reduction reaction. Therefore, the R_p increased when the sintered temperatures were as high as 1250 °C or 1300 °C. The difference in microstructures of the cathode films reflected in the ohmic resistance and polarization resistance (as showed for samples A and E–G in Table 1). JØrgensen et al. [11] reported that R_s decreases as the sintering temperature increased from 950 °C to 1050 °C. This type of behaviour was ascribed to the improved physical and electrical contact between the LSM particles and the YSZ electrolyte. In this work, the R_s of the sample sintered at 1150 °C was higher than that of sintered at 1200 °C. It can be explained that the lower sintered temperature (1150 °C) resulted in a loose structure (Fig. 4(a)). The physical contact between LSM particles and YSZ electrolyte was not ideal which resulted in the increase of R_s. The ohmic resistance R_s was found to increase with temperature increasing from 1200 °C to 1300 °C. Higher than 1200 °C, the effect of formation of low-conductive La-zirconate at the interface between LSM cathode and YSZ electrolyte resulted in the increase of R_s [21]. The changing trend of R_p was the same as the R_s. The R_p of the sample sintered at 1200 °C was the lowest among all samples and the R_p increased when temperature went higher. The R_p of the sample sintered at 1150 °C was higher than 1200 °C (Table 1). Fig. 5 showed the curves of R_{ct} and R_d as a function with different sintering temperature. Similarly, the R_{ct} and R_d were the

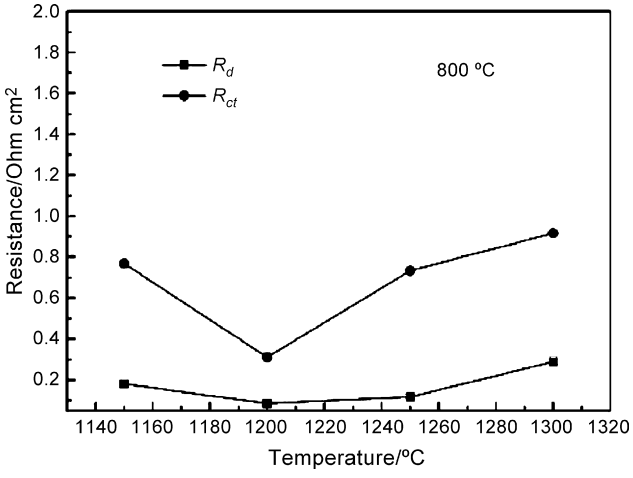

Fig. 5. Resistance change as a function with different temperatures. The resistance was obtained from the impedance measurement made at 800 °C in air.

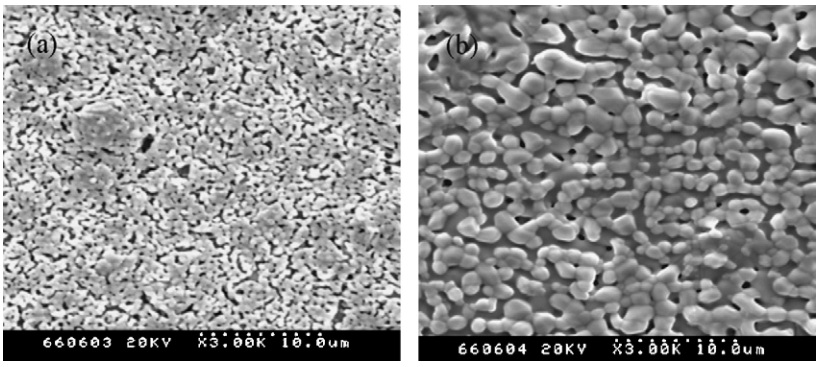

Fig. 6. SEM photos of LSM cathode films sintered at 1200 °C for different time: (a) 1 h, (b) 3 h.

lowest when sintering temperature was 1200 °C (sample A). R_{ct} and R_d of the sample E (sintered at 1150 °C) was higher than that of sample A. After 1200 °C, R_{ct} and R_d increased as temperature went up. This was a result of the loose contact between the particles in the film for sample E which caused the decrease of contact area, leading to the decrease in electrochemical reaction area and the R_{ct} subsequently increased. The partial density film and partial aggregate LSM particles after 1200 °C resulted in the decrease of oxygen reaction area and reduced the porosity. This was the reason why the R_{ct} and R_d increased after 1200 °C.

Microstructure of cathode film is affected not only by the sintering temperature but also by the sintering time. Performance of the cathodes film, fabricated by different sintering time (sample A, H and I), were studied while keeping the sintering temperature at 1200 °C. As shown in Table 1, the R_p of the sample that sintered at 1200 °C for 2 h was the lowest among all the samples. The film sintered at 1200 °C for 1 h (sample H) showed the higher porosity and smaller particles, which should result in lower R_p-values [11]. However, the sample H showed higher R_p-values compared with that of sintered for 2 h. The reason was that the physical contact between LSM particles and YSZ electrolyte of the film sintered at 1200 °C for 1 h was not good (Fig. 6(a)), resulting in the increase of R_s and R_p. The sample sintered for 3 h were over-sintered. The LSM particles were larger than those sintered for 1 h and 2 h and LSM particles were also inhomogeneous, which decreased the electrochemical performance. The R_p of sample H was 1.09 Ω cm^2 and that of sample I was 0.76 Ω cm^2. As for the sample of sintered 2 h, R_p was 0.39 Ω cm^2.

3.4. Performance of LSM–YSZ composite cathode

The total oxygen reduction reaction (ORR) requires the presence of gaseous oxygen and good electronic conductivity in the electrode material as well as the possibility for creating oxide ions to be transported away from reaction site into the bulk of the electrolyte [22]. The triple phase boundary between electrode, electrolyte and gas phase in the bulk of the electrode can meet this standard. For composite cathode, it is conceivable that polarization resistance can be decreased by virtue of extending the TPB sites into the cathode layer [23]. For pure LSM cathode film prepared in this work, good interface structure between the LSM and YSZ were obtained by using the optimized process parameters. Thus, we considered the optimized process parameters discussed above (ethyl cellulose as binder, 120 mesh screen-printing, sintered at 1200 °C for 2 h) were also suitable for LSM–YSZ composite cathode. LSM–YSZ (80 wt% LSM and 20 wt% YSZ) composite cathodes were also prepared by the optimized process parameters. The YSZ (Tosoh) powders was consisted 30 wt% sintered at 700 °C for 2 h (mean particles 0.8 μm) and 70 wt% un-sintered YSZ (particle size <100 nm). The mean particle size of LSM powders (prepared by co-precipitation method) was 0.55 μm. The fine YSZ particles could fill in the gap between LSM and YSZ and coat the LSM particles. Using the fine YSZ particles in a composite cathode can extend the TPB length and retard the growth of the LSM particles, thus increasing the performance and stability of the LSM. The microstructure, electrochemical performance and stability of LSM–YSZ composite cathode were also investigated.

The surface and cross-section SEM photos of the LSM–YSZ composite cathode were shown in Fig. 7. A distinct feature of the LSM–YSZ composite cathode film was homogeneous network as shown in Fig. 7(a), the surface photo of LSM–YSZ composite cathode. The network was beneficial for the electron and ion transport, which will decrease the cathodic polarization. The porosity (about 40%) meets the requirement for gas transportation. From the cross-section photo of LSM–YSZ composite cathode (Fig. 7(b)), it can be found that the LSM–YSZ cathode and the YSZ electrolyte attached very well. The thickness of the composite cathode was approximate 10 μm. Homogeneous distribution of particles and pores showed throughout the whole electrode thickness and surface. Fig. 8 showed the impedance spectra plots and the fitting curves for LSM–YSZ composite cathode at different temperatures. The equivalent circuit $LR_s(QR_{ct})(CR_d)$ was showed in Fig. 8. L is attributed to high-frequency artifacts arising from the measurement apparatus. R_s is the ohmic resistance of electrolyte and lead wires [13]. The high-frequency arc is ascribed to charge-transfer resistance (R_{ct}) from the electrode/YSZ interface into the YSZ electrolyte and the low-frequency arc to the diffusion resistance (R_d) [20,21]. Q is the constant phase element and C represents capacitance. Best fits to all of these data showed two arcs from 750 °C to 800 °C, showing that under cathodic polarization the kinetic processes of the oxygen reduction are controlled not only by charge-transfer but also by adsorption/desorption and diffusion of oxygen. This corresponds to the fact that the oxy-

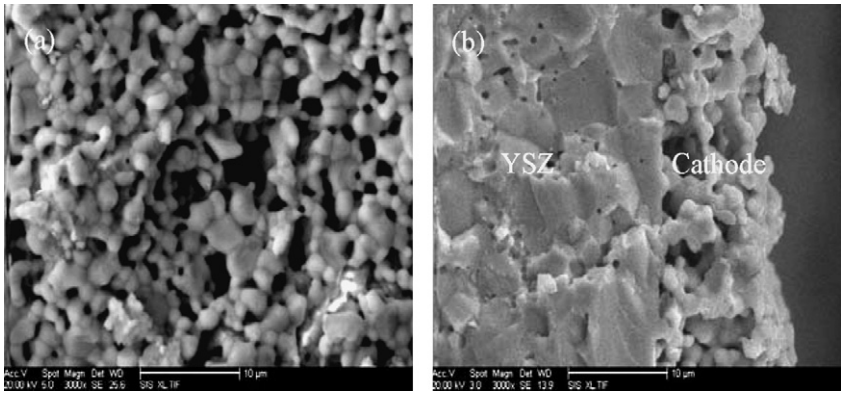

Fig. 7. SEM photos of LSM–YSZ composite cathode: (a) surface, (b) cross-section.

Table 2
Parameters obtained by fitting AC impedance curves for LSM–YSZ composite cathode at different temperatures

T (°C)	R_s ($\Omega\,cm^2$)	R_{ct} ($\Omega\,cm^2$)	R_d ($\Omega\,cm^2$)	R_p ($\Omega\,cm^2$)
750	1.435	0.4183	0.0985	0.5168
800	0.7088	0.2077	0.0386	0.2463
850	0.592	0.1687	0.034	0.2027

gen reduction reaction is achieved through reaction steps such as adsorption, dissociation, diffusion and charge transfer [24]. From Fig. 8 and the data (Table 2), it can be found that the high-frequency arc is larger than the low-frequency arc from 750 °C to 850 °C. As the temperature increased, both R_s and R_{ct} values of LSM–YSZ composite cathode decreased significantly and the sizes of high-frequency arc (QR_{ct}) and low-frequency arc gradually decreased. The decrease of R_{ct} was significant compared with that of R_d. It also showed that the diffusion resistance R_d was similar at 800 °C and 850 °C, which typically indicates that the charge-transfer processes was the rate-limiting step in the cathode reaction. In our study, the LSM–YSZ composite cathode displays a R_p value of 0.2027 $\Omega\,cm^2$ at 850 °C, 0.2463 $\Omega\,cm^2$ at 800 °C and 0.5168 $\Omega\,cm^2$ at 750 °C. Murray and Barnett [13] reported that the polarization resistance of LSM-GDC50 and LSM–YSZ50 composite cathode at 750 °C under open circuit

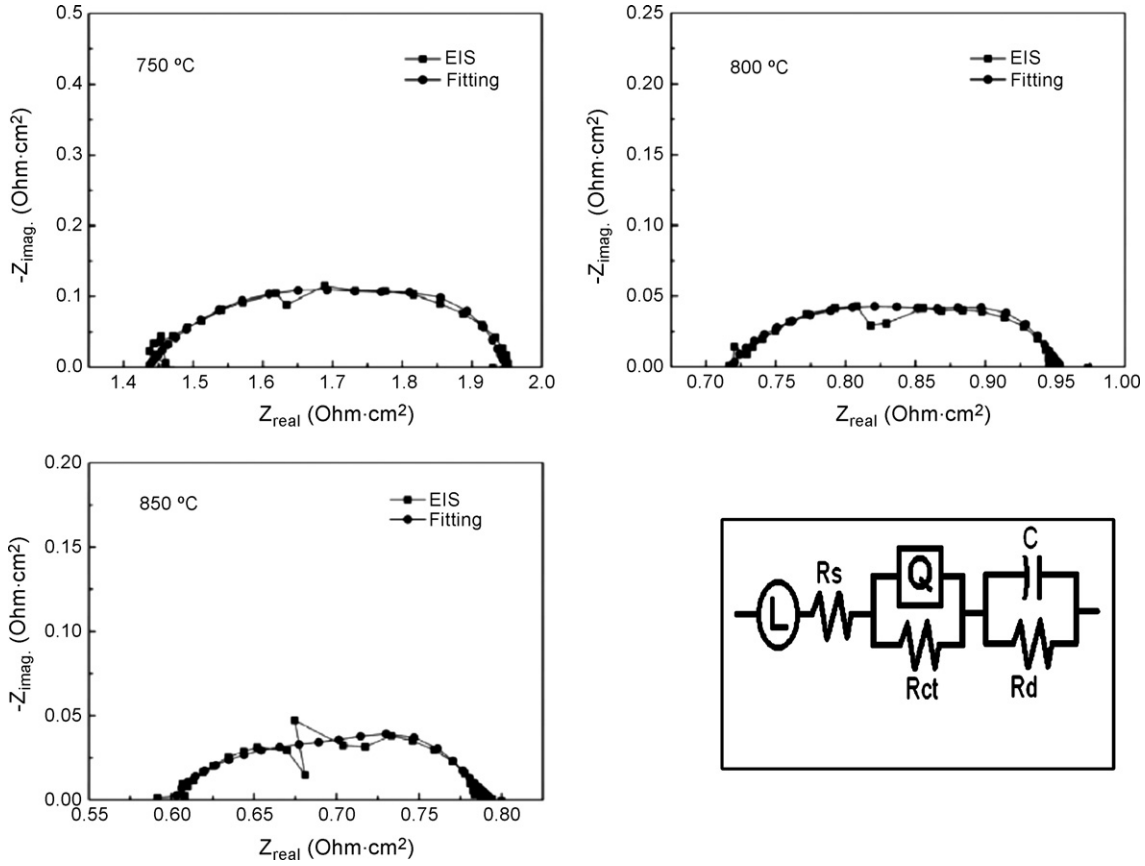

Fig. 8. Impedance spectra measured under open circuit condition at different temperatures in air for LSM–YSZ composite cathode.

on YSZ electrolyte substrates were 0.49 Ω cm^2 and 1.31 Ω cm^2, respectively. It is apparent that the optimized process parameters of fabricating cathode film were suitable not only for pure LSM cathode but also for preparing the LSM–YSZ composite cathode.

The stability is one of the criterions for electrode materials and as well as the microstructure of electrode. Choi et al. [7] reported that fine grain LSM (mean diameter of 1.54 μm) cathode showed good activity in the initial stage, but its activity rapidly declined. Choi et al. [8] also reported the inferior long-term stability of the pure LSM electrode, which ascribed to a faster grain growth of the LSM component and the adding of a YSZ component to LSM electrode layer, which could suppress the particle growth. They also reported that the charge transfer resistance of the LSM–YSZ composite cathode persisted for a longer period of time (no evident variety in 100 h at 900 °C). The stability of LSM–YSZ composite cathode was investigated. Fig. 9 showed the over-potential change of LSM–YSZ composite cathode as a function of cathodic current passage time at 300 mA cm^{-2} and 800 °C. Over-potential was obtained from the galvanostatic step under a constant current density of 300 mA cm^{-2} and 800 °C. It was discovered that the over-potential of LSM–YSZ composite cathode decreased continuously from 420 mV to 98 mV until being polarized at 300 mA cm^{-2} and 800 °C for 150 h. After 150 h, the decreased trend was not evident. This result agreed with the report of Jiang and Love [25] that cathodic current passage markedly reduced the over-potential and improved the electrode reactivity for O_2 reduction reactions. Lee et al. [26] attributed the effect of the cathodic polarization on the polarization of LSM electrode to the formation of oxygen vacancies. The breakdown or the reduction of the resistive lanthanum zirconate ($La_2Zr_2O_7$) phases formed at LSM/YSZ electrolyte interface under cathodic polarization could also contribute to the activation effect of cathodic polarization treatment. Zhang et al. [27] reported that manganese oxide reacts with lanthanum zirconate ($La_2Zr_2O_7$) phase originally existed on the zirconia surface to form the cubic zirconia solid solution of (Zr, La, Mn)O_2 with La dissolved in the solid solution. Jiang and Love [25] reported that the over-potential of LSM decreased from 279 mV to 52 mV after the cathodic current passage at 500 mA cm^{-2} and 1000 °C for 3 h. It was evident that the decrease of over-potential in our work was not quick as compared with the report from Jiang and Love [25]. Jiang and Love [25] also reported that the structural or morphological change caused by the cathodic polarization could contribute to the improvement of the cathodic polarization performance of the LSM cathodes. They also reported that after polarization at 250 mA cm^{-2} and 1000 °C for 57 days, there was little change in the microstructure and morphology of the LSM electrodes. We suggest that the reason of the slow rate of improving performance here was due to the relative low cathodic current density used.

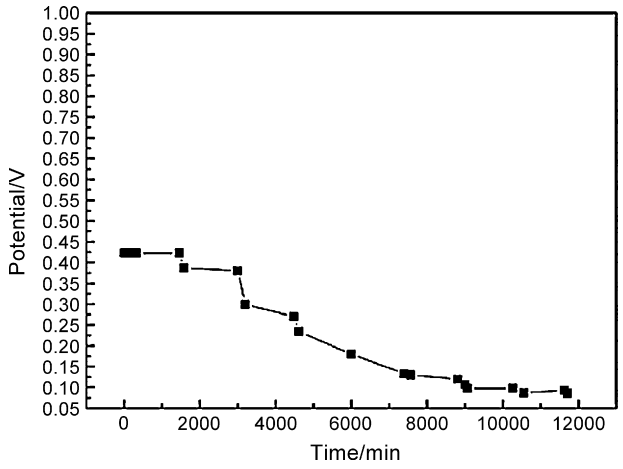

Fig. 9. Over-potential of LSM–YSZ composite cathode as a function of cathodic current passage time at 300 mA cm^{-2} and 800 °C in air.

Next step that need to be taken is to study the relationship between the microstructure and the long-term stability of LSM–YSZ composite cathodes under SOFC operating conditions.

4. Conclusion

Four important process parameters including the selection of binders, the mesh of screen, sintering temperature and sintering time were investigated. The conclusions were obtained as following: (a) the binders used in preparing the screen-printing slurry greatly influenced the microstructure of the screen-printed cathode films. Using the ethyl cellulose as a binder to prepare the cathode film, we found that pore size distribution was homogeneous. The film using polyvinyl-butyral as binder was dense and the porosity was low. This could be a result of the ethyl cellulose being a linear polymer, while polyvinyl-butyral has branches in its structure. Ethyl cellulose was the preferable binder to obtain fine and uniform microstructures due to the linear structure; (b) to obtain porous cathode films, the mesh amount of screen should be suitable. The films of 100 mesh and 140 mesh screen possessed inhomogeneous pores compared with the film made by 120 mesh screen. The cathode film made by 120 mesh screen possessed the lowest polarization resistance; (c) the microstructure of the electrodes was strongly affected by both the sintering temperature and sintering time. The R_{ct} and R_d were the lowest when sintering temperature was 1200 °C compared with 1150 °C, 1250 °C and 1300 °C. The film sintered at 1200 °C for 2 h owned to its high porosity, small particles and good physical contact between LSM particles and YSZ electrolyte, which resulted in low R_p-values and interface resistance. These process parameters were also suitable for LSM–YSZ composite cathode. The LSM–YSZ composite cathode prepared by the optimized process parameters possessed homogeneous network structure and favorable porosity (40%). The LSM–YSZ composite cathode displays a R_p value of 0.2027 Ω cm^2 at 850 °C, 0.2463 Ω cm^2 at 800 °C and 0.5168 Ω cm^2 at 750 °C. The performance of the LSM–YSZ composite cathode improved significantly after being polarized at 300 mA cm^{-2} and 800 °C till 150 h. The over-potential of the composite cathode was stable after 150 h. Therefore, it was concluded that the optimized process parameters (ethyl cellulose as binder, 120 mesh screen, sintered at 1200 °C for 2 h) using screen-printing was suitable

not only for the preparation of LSM cathode but also for the preparation of LSM–YSZ composite cathode films.

Acknowledgement

The project is financially supported by 863 National Project (2003 AA302440).

References

[1] Y.-K. Lee, J.-Y. Kim, Y.-K. Lee, I. Kim, H.-S. Moon, J.-W. Park, C.P. Jacobson, S.J. Visco, J. Power Sources 115 (2003) 219–228.
[2] W.G. Wang, Y.-L. Liu, R. Barfod, S.B. Schougaard, Electrochem. Solid-State Lett. 8 (12) (2005) A619–A621.
[3] J.Y. Kim, V.L. Sprenkle, N.L. Canfield, K.D. Meinhardt, L.A. Chick, J. Electrochem. Soc. 153 (5) (2006) A880–A886.
[4] K.T. Lee, D.M. Bierschenk, A. Manthiram, J. Electrochem. Soc. 153 (7) (2006) A1255–A1260.
[5] L.-W. Tai, M.M. Nasrallah, H.U. Anderson, D.M. Sparlin, S.R. Sehlin, Solid State Ionics 76 (1995) 273–283.
[6] E.P. Murray, M.J. Sever, S.A. Barnett, Solid State Ionics 148 (2002) 27–34.
[7] J.H. Choi, J.H. Jang, J.H. Ryu, S.M. Oh, J. Power Sources 87 (2000) 92–100.
[8] J.H. Choi, J.H. Jang, S.M. Oh, Electrochim. Acta 46 (2001) 867–874.
[9] S. de Souza, S.J. Visco, L.C. de Jonghe, Solid State Ionics 98 (1997) 57–61.
[10] T. Kenjo, M. Nishiya, Solid State Ionics 57 (1992) 295–302.
[11] M.J. JØrgensen, S. Primdahl, C. Bagger, M. Mogensen, Solid State Ionics 139 (2001) 1–11.
[12] S. Wang, Y. Jiang, Y. Zhang, J. Yan, W. Li, Solid State Ionics 113–115 (1998) 291–303.
[13] E.P. Murray, S.A. Barnett, Solid State Ionics 143 (2001) 265–273.
[14] T. Tsai, S.A. Barnett, Solid State Ionics 93 (1997) 207–219.
[15] M.J.L. Østergard, C. Clausen, C. Bagger, M. Mogensen, Electrochim. Acta 40 (12) (1995) 1971–1981.
[16] H.S. Song, W.H. Kim, S.H. Hyun, J. Moon, J. Kim, H.-W. Lee, J. Power Sources 167 (2007) 258–264.
[17] D. Kek, P. Panjan, E. Wanzenberg, J. Eur. Ceram. Soc. 21 (2001) 1861–1865.
[18] Y. Matsuzaki, I. Yasuda, Solid State Ionics 126 (1999) 307–313.
[19] K.J. Yoon, W. Huang, G. Ye, S. Gopalan, U.B. Pal, D.A. Seccombe Jr., J. Electrochem. Soc. 154 (2007) B389–B395.
[20] A. Mitterdorfer, L.J. Gauckler, Solid State Ionics 111 (1998) 185–218.
[21] H.Y. Lee, S.M. Oh, Solid State Ionics 90 (1996) 133–140.
[22] M.J. JØrgensen, S. Primdahl, M. Mogensen, Electrochim. Acta 44 (1999) 4195–4201.
[23] X.D. Zhu, K.N. Sun, N.Q. Zhang, X.B. Chen, L.J. Wu, D.C. Jia, Electrochem. Commun. 9 (2007) 431–435.
[24] E.P. Murray, T. Tsai, S.A. Barnet, Solid State Ionics 110 (1998) 235–243.
[25] S.P. Jiang, J.G. Love, Solid State Ionics 158 (2003) 45–53.
[26] H.Y. Lee, W.S. Cho, S.M. Oh, H.-D. Wiemhöfer, W. Göpel, J. Electrochem. Soc. 142 (1995) 2659–2664.
[27] J.-P. Zhang, S.P. Jiang, K. Foger, in: S.C. Singhal, M. Dokiya (Eds.), Solid Oxide Fuel Cells-VI, PV99-19, The Electrochemical Soc., Pennington, NJ, 1999, pp. 962–971.